Hindawi
Mathematical Problems in Engineering
Volume 2021, Article ID 8840244, 18 pages
https://doi.org/10.1155/2021/8840244

*Research Article*

# Novel Nonsingular Fast Terminal Sliding Mode Control for a Class of Second-Order Uncertain Nonlinear Systems

**Huihui Pan [1,2] and Guangming Zhang [1]**

[1]*School of Mechanical and Power Engineering, Nanjing Tech University, Nanjing 211816, China*
[2]*College of Electrical Engineering, Tongling University, Tongling 244061, China*

Correspondence should be addressed to Guangming Zhang; zgm@njtech.edu.cn

Received 28 August 2020; Revised 18 December 2020; Accepted 2 January 2021; Published 28 January 2021

Academic Editor: Kai Zhang



This paper presents a novel nonsingular fast terminal sliding mode control scheme for a class of second-order uncertain nonlinear systems. First, a novel nonsingular fast terminal sliding mode manifold (NNFTSM) with adaptive coefficients is put forward, and a novel double power reaching law (NDP) with dynamic exponential power terms is presented. Afterwards, a novel nonsingular fast terminal sliding mode (NNFTSMNDP) controller is designed by employing NNFTSM and NDP, which can improve the convergence rate and the robustness of the system. Due to the existence of external disturbances and parameter uncertainties, the system states under controller NNFTSMNDP cannot converge to the equilibrium but only to the neighborhood of the equilibrium in finite time. Considering the unsatisfying performance of controller NNFTSMNDP, an adaptive disturbance observer (ADO) is employed to estimate the lumped disturbance that is compensated in the controller in real-time. A novel composite controller is presented by combining the NNFTSMNDP method with the ADO technique. The finite-time stability of the closed-loop system under the proposed control method is proven by virtue of the Lyapunov stability theory. Both simulation results and theoretical analysis illustrate that the proposed method shows excellent control performance in the existence of disturbances and uncertainties.

## 1. Introduction

Sliding mode control (SMC) is a popular method to control nonlinear systems owing to its simplicity and strong robustness [1–6]. Among the SMC category, the research studies on terminal sliding mode control (TSMC) have received considerable attention. TSMC adopts terminal sliding mode manifold that can drive the system states converge to the equilibrium within finite time, and it has been widely utilized in many physical systems [7–10], such as spacecrafts, robots, and permanent magnet synchronous motors.

As known, the standard TSM has two disadvantages. One is that it has slower convergence rate than the linear sliding mode (LSM) when the system states are far away from the equilibrium point. To solve the problem, fast terminal sliding mode (FTSM) combining the advantages of LSM and TSM was given in [11]. The other one is the singularity problem. The singularity may occur due to the presence of the negative exponential term. To remedy the problem, there are many methods that have been presented. For instance, one approach is to switch the TSM to a general sliding surface, when the states enter the region near the origin [12, 13]. Another approach is to design a new form of TSM with nonsingularity known as nonsingular TSM (NTSM) [14, 15]. Concerning the aforementioned two problems, the scholars have done a lot of studies. In [16], a new type of NTSM has been developed by switching the system dynamic from an LSM to an NTSM, which can obtain global fast convergence rate. A novel NFTSM has been designed, which has the properties of the fast convergence and nonsingularity [17]. A novel exponential fast NTSM has been given in [18], which can improve the convergence rate. As can be seen from the existing literature studies, most of the TSM control approaches were presented for second-order systems. The authors in [19, 20] proposed the recursive TSM control strategy, which can be applicable to higher-order systems. It is noted that the parameters of most of the TSM controllers are fixed in the whole control process so that the optimal dynamic performance of the system cannot be achieved.

TSMC exhibits good control performance in many nonlinear systems. Nevertheless, the chattering problem cannot be ignored [21]. To this end, many methods have been presented to reduce the chattering. As we know, TSMC based on the reaching law is an effective strategy to alleviate the chattering. There are some conventional reaching laws that have been designed, such as the constant-proportional rate reaching law [22], the quick power reaching law [23], and the double power reaching law [24]. Besides, some novel reaching laws have also been developed to ensure the fast reaching convergence to the sliding surface [25–29]. Among them, the double power reaching law can obtain excellent reaching performance, which is widely used in the SMC design. However, when a large initial error exists or when the system states are far away from the sliding surface, it is unable to guarantee sufficiently fast error convergence.

Previous studies have proposed different TSMCs and have important significance. In fact, how to enhance the convergence rate and reduce the chattering is still valuable for further research. The motivation of this paper is to present a novel control scheme for second-order systems to improve the control performance. A novel NTSM with adaptive coefficients and a novel double power reaching law with dynamic power terms are developed in this paper.

It is worthwhile noting that there may exist various disturbances in the practical engineering systems [30, 31]. In recent years, the disturbance observer-based methods are applied to counteract disturbances [32–36]. In these methods, the disturbance is estimated by a disturbance observer, and its estimation is compensated in the controller online. Furthermore, the disturbance observer can be utilized to alleviate the chattering [37, 38]. In the most existing references, it is assumed that the upper bounds of the lumped disturbance and its derivatives are known. However, this information is usually difficult to be acquired in practical systems. An adaptive disturbance observer (ADO) proposed in our previous study [39] can guarantee the observer error converging to zero in finite time and do not require the knowledge about the lumped disturbance and its derivatives. In this paper, the ADO is employed to obtain the estimation of disturbances and uncertainties.

According to the above discussion and our previous study in [39], a novel disturbance observer-based nonsingular fast terminal sliding mode control method is proposed for a class of second-order uncertain nonlinear systems to enhance the convergence rate and control accuracy. The main contributions of this paper are summarized as follows:

(1) A novel nonsingular fast terminal sliding mode manifold (NNFTSM) with adaptive coefficients is proposed, which can enhance the effect of the major term and weaken the effect of the secondary term at different stages to further speed up the convergence rate of the system states to the equilibrium point.

(2) A novel double power reaching law (NDP) with two variable exponential power terms is proposed, which can adaptively adjust two exponential parameters in the different stages so that the system trajectory arrives at the sliding surface with less time.

(3) The NNFTSMNDP controller combining NNFTSM and NDP is designed, which can force the system states more quickly converge to the neighborhood of the equilibrium in finite time compared to conventional NFTSMDP controller.

(4) A novel composite control strategy is presented by combining the NNFTSMNDP method with the ADO technique, which can guarantee that the system states are fast convergent to the equilibrium without the knowledge about the upper bounds of the lumped disturbance and its derivatives. Comparative simulation results illustrate that the proposed NNFTSMNDP-ADO obtains better control performance in comparison with NFTSMDP-ADO and the method of [40].

This paper is structured as follows: Section 2 provides some useful lemmas. The control methods and the stability analysis are introduced in Section 3. The application of the proposed NNFTSMNDP-ADO control scheme to a two-link rigid robotic manipulator is presented in Section 4. Section 5 is the conclusion.

Throughout the paper, $\text{sig}(\cdot)^{\alpha} = |\cdot|^{\alpha}\text{sign}(\cdot)$ for any $\alpha > 0$.

## 2. Mathematical Preliminaries

Consider a class of typical second-order nonlinear systems with the following description:

$$\begin{cases} \dot{x}_1 = x_2, \\ \dot{x}_2 = a(x) + b(x)u + d, \end{cases} \tag{1}$$

where $a(x)$ and $b(x)$ denote smooth nonlinear functions of $x$. $d$ represents lumped disturbance including parameter perturbation and external disturbance.

*Assumption 1.* The magnitude of $d$ is bounded such that $|d| < D_0$. The first-order and second-order derivatives of $d$ exist and satisfy that $|\dot{d}| < D_1$, $|\ddot{d}| < D_2$, where the bounds $D_0$, $D_1$, and $D_2$ are unknown positive numbers.

**Lemma 1** (see [41]). *Consider the following nonlinear system:*

$$\begin{aligned} \dot{x} &= f(x), \\ x(0) &= x_0, \end{aligned} \tag{2}$$

*where $x \in R^n$ and $f(x)$: $D \longrightarrow R^n$ is continuous on an open neighborhood $D \subseteq R^n$ of the origin, and $f(0) = 0$. Suppose that there is a positive and differentiable function $V(x)$: $R^n \longrightarrow R$, and there are real numbers $c > 0$ and*

$0 < \mu < 1$ *satisfying that* $\dot{V}(x) \leq -cV^{\mu}(x)$. *Then, the origin of system (2) is finite-time stable.*

**Lemma 2** (see [42]). *Suppose that there is a continuous function* $V\colon R^n \longrightarrow R$ *satisfying that* $V(0) = 0$, *and the origin is the equilibrium point. If the numbers* $0 < \vartheta < 1$, $\varsigma > 0$, $r_\vartheta > 0$, *and* $r_\varsigma > 0$ *and the following inequality*

$$\dot{V} \leq \begin{cases} -r_\vartheta V^{1-\vartheta}, & V \leq 1, \\ -r_\varsigma V^{1+\varsigma}, & V \geq 1, \end{cases} \tag{3}$$

*holds, then the zero solution of system (2) is fixed-time stable. The maximum convergence time can be estimated by*

$$T(x) \leq \frac{1}{\vartheta r_\vartheta} + \frac{1}{\zeta r_\varsigma}. \tag{4}$$

## 3. Control Methods and Stability Analysis

In this section, the control methods and the stability analysis are presented.

*3.1. Novel NFTSM Design.* For (1), to guarantee that the system states can quickly converge to the origin, a novel nonsingular fast terminal sliding mode manifold (NNFTSM) is proposed as

$$s = k_1' x_1 + k_2' \operatorname{sig}(x_1)^{\gamma_1} + \operatorname{sig}(x_2)^{\gamma_2}, \tag{5}$$

with

$$\begin{aligned} k_1' &= \frac{2k_1}{1 + e^{c_1(|x_1| - \nu)}}, \\ k_2' &= \frac{2k_2}{1 + e^{-c_2(|x_1| - \nu)}}, \end{aligned} \tag{6}$$

in which $k_1 > 0$, $k_2 > 0$, $c_1 > 0$, $c_2 > 0$, $\gamma_1 > \gamma_2$, $1 < \gamma_2 < 2$, and $\upsilon = (k_1/k_2)^{1/(\gamma_1 - 1)}$.

When NNFTSM $s = 0$, the system dynamic along sliding surface (5) can be expressed by

$$x_2 = -\left(k_1'|x_1| + k_2'|x_1|^{\gamma_1}\right)^{(1/\gamma_2)} \operatorname{sign}(x_1). \tag{7}$$

When the system state $x_1$ is far from the origin, the term $k_2' \operatorname{sig}(x_1)^{\gamma_1}$ plays a major role in NNFTSM (5). Then, (7) can be approximately described as

$$x_2 = -\left(k_2'|x_1|^{\gamma_1}\right)^{(1/\gamma_2)} \operatorname{sign}(x_1). \tag{8}$$

When the system state $x_1$ is close to the origin, the term $k_1' x_1$ plays a major role in NNFTSM (5). Then, (7) can be approximately described as

$$x_2 = -\left(k_1'|x_1|\right)^{(1/\gamma_2)} \operatorname{sign}(x_1). \tag{9}$$

According to (6), the coefficients in NNFTSM are the exponential functions of the state $x_1$. This can achieve the adaptivity to enhance the effect of the major term and weaken the effect of the secondary term in the different stages, which is helpful for speeding up the convergence rate of the system.

According to the above, one can know that the proposed NNFTSM has fast convergence rate. To verify this result, the conventional NFTSM is given as comparison:

$$s = x_1 + k \operatorname{sig}(x_1)^{\gamma_1} + \beta \operatorname{sig}(x_2)^{\gamma_2}, \tag{10}$$

where $k > 0$, $\beta > 0$, $\gamma_1 > \gamma_2$, and $1 < \gamma_2 < 2$.

For a relatively fair comparison, the parameters in (5) and (10) are set as $k_1 = k_2 = 1$, $k = \beta = 1$, $\gamma_1 = 2$, $\gamma_2 = 1.4$, $c_1 = c_2 = 2$, and $\nu = 1$. The initial state is set as $x_1(0) = 0.8$, $x_1(0) = 30$, respectively. Figure 1 illustrates the dynamic performances of the two siding mode manifolds. It can be seen that the proposed NNFTSM has faster convergence performance than the conventional NFTSM, whether the state is far from or close to the origin.

*3.2. Novel Double Power Reaching Law.* Generally, the double power reaching law can be expressed as

$$\dot{s} = -\lambda_1 \operatorname{sig}(s)^{\psi_1} - \lambda_2 \operatorname{sig}(s)^{\psi_2}, \tag{11}$$

where $\lambda_1 > 0$, $\lambda_2 > 0$, $0 < \psi_1 < 1$, and $\psi_2 > 1$.

To further improve the reaching performance, this paper proposes a novel double power reaching law. Here, a continuous sigmoid function will be used. The sigmoid function is a smooth and strictly monotone function, which can be described as

$$f(x, \theta) = \frac{2}{1 + e^{-\theta x}} - 1. \tag{12}$$

Combining the sigmoid function, a novel double power reaching law (NDP) is put forward as follows:

$$\dot{s} = -\lambda_1 \operatorname{sig}(s)^{\kappa_1} - \lambda_2 \operatorname{sig}(s)^{\kappa_2}, \tag{13}$$

with

$$\kappa_1 = \eta_0 f(s^\sigma, 1) - \eta_1 f\left(s^2, \theta\right) + \eta_2, \tag{14}$$

$$\kappa_2 = 0.5\eta + 0.5 + (0.5\eta - 0.5)\operatorname{sign}(|s| - 1), \tag{15}$$

in which $\sigma$ is a positive even number, $\theta > 0$, $\eta_0 > 1$, $0 < \eta_1 < \eta_2 < 1$, and $\eta = \eta_0 - \eta_1 + \eta_2$.

The novel reaching law has two dynamic power terms that are adaptive to the variation of the sliding variable $s$. $\kappa_1$ is constructed by the sigmoid function. $\kappa_2$ is a piecewise function. By properly choosing parameters $r$ and $\theta$, (13) can be rewritten as follows:

$$\begin{cases} \dot{s} = -\lambda_1 \operatorname{sig}(s)^{\eta} - \lambda_2 \operatorname{sig}(s)^{\eta}, & |s| \geq 1, \\ \dot{s} = -\lambda_1 \operatorname{sig}(s)^{\eta_2 - \eta_1} - \lambda_2 s, & 0 < |s| < 1, \\ \dot{s} = -\lambda_1 \operatorname{sig}(s)^{\eta_2} - \lambda_2 s, & \text{near} |s| = 0. \end{cases} \tag{16}$$

According to (16), when $|s| \geq 1$, both terms play the important role in the reaching law, while when $0 < |s| < 1$, the reaching law changes into a quick power reaching law, so that it can enhance the convergence rate whether the sliding variable $s$ is far from or close to zero. Note that, when $s$ is

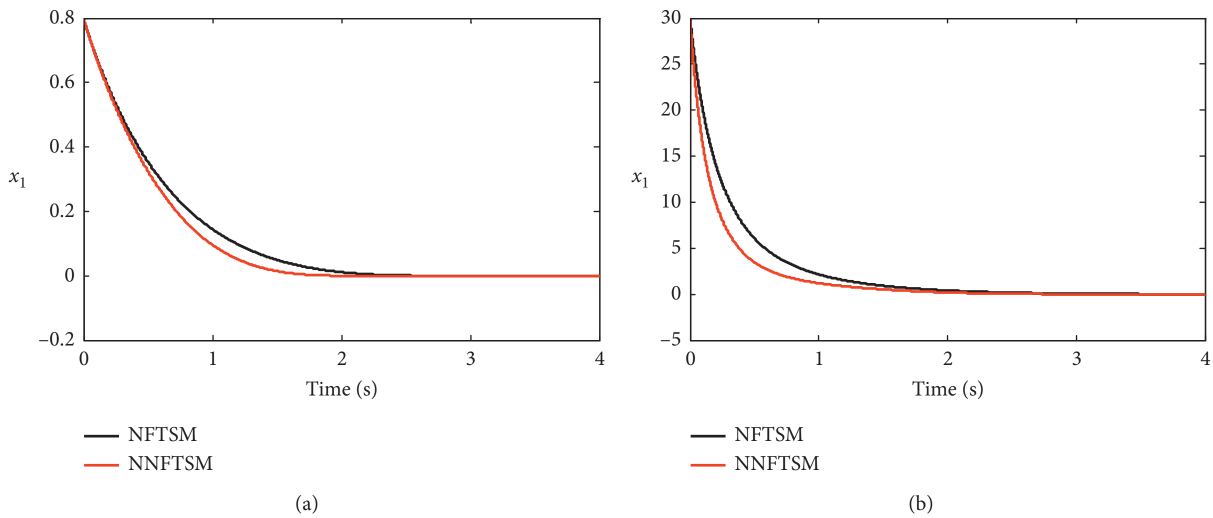


FIGURE 1: Comparison of NNFTSM and NFTSM. (a) $x_1(0) = 0.8$. (b) $x_1(0) = 30$.

near 0, then $|s|^{\eta_2} < |s|^{\eta_2 - \eta_1}$ such that the chattering reduction can be achieved. Therefore, the novel double power reaching law can make the system have excellent dynamic performance in the reaching phase.

For example, set $\eta_0 = 1.4$, $\eta_1 = 0.5$, and $\eta_2 = 0.6$, and the response curves of $\kappa_1$ with different parameters are plotted in Figure 2. With the parameters in (13)–(15) chosen as $\lambda_1 = 5$, $\lambda_2 = 5$, $\eta = 1.5$, $\psi_1 = 0.6$, $\psi_2 = 1.5$, $\sigma = 500$, and $\theta = 800$, the convergence of the two reaching laws under the initial condition $s(0) = 1$ and $s(0) = 200$ is displayed in Figure 3. It can be seen from Figure 3 that the proposed reaching law has faster convergence performance than the conventional double power reaching law.

### 3.3. Controller NNFTSMNDP Design

**Theorem 1.** *For system (1), a novel nonsingular fast terminal sliding mode controller based on the novel double power reaching law (NNFTSMNDP) is designed as*

$$u = -\frac{1}{b(x)}\left[a(x) + \frac{1}{\gamma_2 |x_2|^{\gamma_2 - 1}}\left(k_1' x_2 + \dot{k}_1' x_1 + k_2' \gamma_1 |x_1|^{\gamma_1 - 1} x_2 + \dot{k}_2' \operatorname{sig}(x_1)^{\gamma_1}\right) + \lambda_1 \operatorname{sig}(s)^{\kappa_1} + \lambda_2 \operatorname{sig}(s)^{\kappa_2}\right], \tag{17}$$

*with*

$$\begin{aligned} \dot{k}_1' &= -\frac{2k_1 c_1 e^{c_1(|x_1| - \nu)} x_2 \operatorname{sign}(x_1)}{\left(1 + e^{c_1(|x_1| - \nu)}\right)^2}, \\ \dot{k}_2' &= \frac{2k_2 c_2 e^{-c_2(|x_1| - \nu)} x_2 \operatorname{sign}(x_1)}{\left(1 + e^{-c_2(|x_1| - \nu)}\right)^2}, \end{aligned} \tag{18}$$

*in which s is defined by (5). The system trajectory converges to the neighborhood of NNTSM $s = 0$. And, the system states converge to a small region around the origin.*

*Proof*

*Step 1*. Consider the following Lyapunov function:

$$V_1 = s^2. \tag{19}$$

Taking derivative of (19), there is

$$\dot{V}_1 = 2s\dot{s} = 2s\left(k_1' x_2 + \dot{k}_1' x_1 + k_2' \gamma_1 |x_1|^{\gamma_1 - 1} x_2 + \dot{k}_2' \operatorname{sig}(x_1)^{\gamma_1} + \gamma_2 |x_2|^{\gamma_2 - 1} \dot{x}_2\right). \tag{20}$$

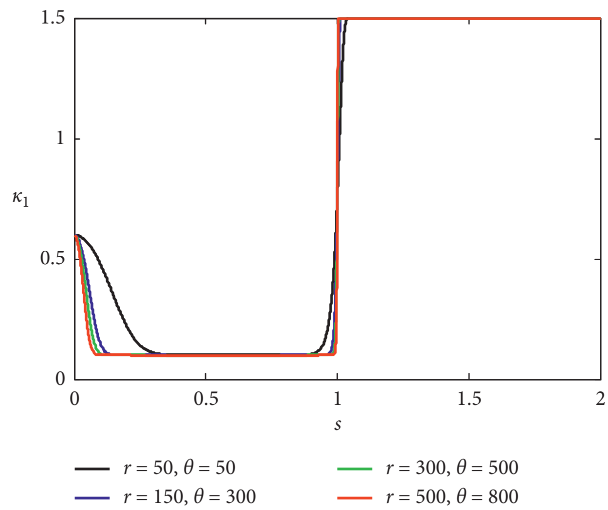


FIGURE 2: The curves of $\kappa_1$ with different parameters.

Substituting control law (17) into (20) yields

$$\begin{aligned}\dot{V}_1 &= 2s\left[k_1'x_2 + \dot{k}_1'x_1 + k_2'\gamma_1|x_1|^{\gamma_1-1}x_2 + \dot{k}_2'\mathrm{sig}(x_1)^{\gamma_1} + \gamma_2|x_2|^{\gamma_2-1}(a(x)+b(x)u+d)\right]\\ &= 2s\left\{k_1'x_2 + \dot{k}_1'x_1 + k_2'\gamma_1|x_1|^{\gamma_1-1}x_2 + \dot{k}_2'\mathrm{sig}(x_1)^{\gamma_1} + \gamma_2|x_2|^{\gamma_2-1}\left[-\frac{1}{\gamma_2|x_2|^{\gamma_2-1}}\left(k_1'x_2 + \dot{k}_1'x_1 + k_2'\gamma_1|x_1|^{\gamma_1-1}x_2 + \dot{k}_2'\mathrm{sig}(x_1)^{\gamma_1}\right)\right.\right.\\ &\qquad \left.\left. - \lambda_1\mathrm{sig}(s)^{\kappa_1} - \lambda_2\mathrm{sig}(s)^{\kappa_2} + d\right]\right\}\\ &= -2\gamma_2|x_2|^{\gamma_2-1}s\left(\lambda_1\mathrm{sig}(s)^{\kappa_1} + \lambda_2\mathrm{sig}(s)^{\kappa_2} - d\right).\end{aligned} \tag{21}$$

Equation (21) can be transformed into the following two equations:

$$\dot{V}_1 = -2\gamma_2|x_2|^{\gamma_2-1}s\left[\lambda_1\mathrm{sig}(s)^{\kappa_1} + (\lambda_2 - \frac{d}{\mathrm{sig}(s)^{\kappa_2}})\mathrm{sig}(s)^{\kappa_2}\right], \tag{22}$$

$$\dot{V}_1 = -2\gamma_2|x_2|^{\gamma_2-1}s\left[\left(\lambda_1 - \frac{d}{\mathrm{sig}(s)^{\kappa_1}}\right)\mathrm{sig}(s)^{\kappa_1} + \lambda_2\mathrm{sig}(s)^{\kappa_2}\right]. \tag{23}$$

In (22), for any $x_2 \neq 0$, when $\lambda_2 - d/\mathrm{sig}(s)^{\kappa_2} > 0$ holds, the stability can be guaranteed. Then, the sliding variable $s$ can converge to a residual set as $|s| \leq (D_0/\lambda_2)^{1/\kappa_2}$. Denote $\lambda_{2*} = \lambda_2\gamma_2|x_2|^{\gamma_2-1}$, and equation (22) turns to

$$\dot{V}_1 \leq -2\lambda_{2*}|s|^{\kappa_1+1} = -2\lambda_{2*}V_1^{((\kappa_1+1)/2)}. \tag{24}$$

Rewrite (24) in the following form as

$$\dot{V}_1 \leq \begin{cases} -2\lambda_{2*}V_1^{((\eta+1)/2)}, & V_1 \geq 1, \\ -2\lambda_{2*}V_1^{((\eta_2+1)/2)}, & V_1 \leq 1. \end{cases} \tag{25}$$

According to Lemma 2, it can be known that the sliding variable $s$ can converge to a bounded region in finite time.

By the similar analysis for (23), $s$ can converge to a residual set as $|s| \leq (D_0/\lambda_1)^{1/\kappa_1}$. Based on the aforementioned analysis, denote $\delta = \min((D_0/\lambda_1)^{1/\kappa_1}, (D_0/\lambda_2)^{1/\kappa_2})$, and the sliding variable $s$ can converge to the following region:

$$|s| \leq \min\left(\left(\frac{D_0}{\lambda_1}\right)^{(1/\kappa_1)}, \left(\frac{D_0}{\lambda_2}\right)^{(1/\kappa_2)}\right) = \delta. \tag{26}$$

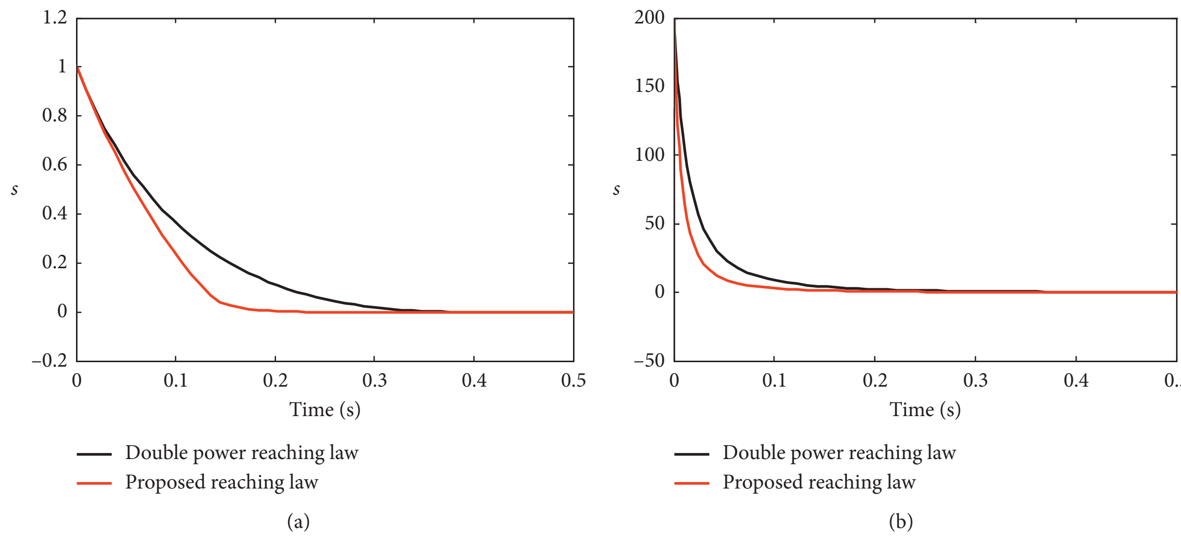


FIGURE 3: The convergence of two reaching laws. (a) $s(0) = 1$. (b) $s(0) = 200$.

Note that, in (21), $x_2 = 0$ may hinder the reachability of NNFTSM (5).

Next, we will illustrate that $x_2 = 0$ is not an attractor in the reaching motion. Substitute control law (17) into system (1), let $x_2 = 0$, and there is

$$\dot{x}_2 = -\lambda_1 \operatorname{sig}(s)^{\kappa_1} - \lambda_2 \operatorname{sig}(s)^{\kappa_2} + d. \tag{27}$$

For any $x_2 = 0$ and $s$ in the outside of region (26), it can be obtained that

$$\dot{x}_2 = \begin{cases} -\left(\lambda_1 - \dfrac{d}{\operatorname{sig}(s)^{\kappa_1}}\right)\operatorname{sig}(s)^{\kappa_1} - \lambda_2 \operatorname{sig}(s)^{\kappa_2} \neq 0, \\ -\lambda_1 \operatorname{sig}(s)^{\kappa_1} - \left(\lambda_2 - \dfrac{d}{\operatorname{sig}(s)^{\kappa_2}}\right)\operatorname{sig}(s)^{\kappa_2} \neq 0. \end{cases} \tag{28}$$

Thus, in the case of $x_2 = 0$, the reachability of NNFTSM (5) can be still guaranteed.

*Step 2.* According to $|s| \le \delta$, there is

$$s = k_1' x_1 + k_2' \operatorname{sig}(x_1)^{\gamma_1} + \operatorname{sig}(x_2)^{\gamma_2}, \quad |s| \le \delta. \tag{29}$$

For (29), the following two forms can be obtained:

$$\operatorname{sig}(x_2)^{\gamma_2} + \left(k_1 - \frac{s\left(1 + e^{c_1(|x_1| - \nu)}\right)}{2x_1}\right)\frac{2x_1}{1 + e^{c_1(|x_1| - \nu)}} + k_2' \operatorname{sig}(x_1)^{\gamma_1} = 0, \tag{30}$$

$$\operatorname{sig}(x_2)^{\gamma_2} + k_1' x_1 + \left(k_2 - \frac{s\left(1 + e^{-c_2(|x_1| - \nu)}\right)}{2\operatorname{sig}(x_1)^{\gamma_1}}\right)\frac{2\operatorname{sig}(x_1)^{\gamma_1}}{1 + e^{-c_2(|x_1| - \nu)}} = 0. \tag{31}$$

When $k_1 - s(1 + e^{c_1(|x_1| - \nu)})/(2x_1) > 0$ holds, (30) will still maintain the NNFTSM form as (5). That is to say, the system trajectory will persistently converge to the proposed NNFTSM until it satisfies $k_1 - s(1 + e^{c_1(|x_1| - \nu)})/(2x_1) \le 0$. Thus, we can get

$$\frac{|x_1|}{1 + e^{c_1(|x_1| - \nu)}} \le \frac{\delta}{2k_1}. \tag{32}$$

Then, the state $x_1$ will converge into the following region in finite time:

$$|x_1| \le \frac{\delta}{k_1}. \tag{33}$$

Likewise, from (31), it can be easily obtained that

$$\frac{|x_1|^{\gamma_1}}{1+e^{-c_2(|x_1|-\nu)}} \le \frac{\delta}{2k_2}. \tag{34}$$

Then, combining (32) and (34), it can be obtained that

$$|x_2|^{\gamma_2} \le |s| + \frac{2k_1|x_1|}{1+e^{c_1(|x_1|-\nu)}} + \frac{2k_2|x_1|^{\gamma_1}}{1+e^{-c_2(|x_1|-\nu)}} \le 3\delta. \tag{35}$$

So,

$$|x_2| \le (3\delta)^{1/\gamma_2}. \tag{36}$$

Accordingly, the proof shows that the closed-loop control system is stable, and the system states can converge to a small region $R = \{(x_1, x_2)\colon |x_1| \le \delta/k_1, |x_2| \le (3\delta)^{1/\gamma_2}\}$ near zero. This completes the proof. □

*Remark 1.* In the NNFTSMNDP algorithm, the conventional NFTSM and double power reaching law (DP) are improved to make the control system obtain faster convergence rate in both the reaching phase and the sliding phase.

*Remark 2.* Note that controller NNFTSMNDP cannot ensure that the system states strictly converge to the equilibrium point but only to the neighborhood of the equilibrium point due to the affection of disturbances and uncertainties. The control method can be used when the control precision is required to be not high.

*3.4. Controller NNFTSMNDP-ADO Design.* The NNFTSMNDP-ADO algorithm consists of two parts. First, the ADO is employed to estimate the lumped disturbance within finite time. Second, the disturbance estimation obtained from the ADO is compensated in the controller to suppress the disturbance. The proof for the finite-time stability of the closed-loop system under the proposed control method is also given in this subsection.

According to our previous research in [39], the ADO is introduced for system (1):

$$\begin{cases} \alpha = z - x_2, \\ \Omega = \dot{\alpha} + k_3 \mathrm{sig}(\alpha)^{\psi_3} + k_4 \mathrm{sig}(\alpha)^{\psi_4}, \\ \dot{z} = a(x) + b(x)u + \hat{d} - k_3 \mathrm{sig}(\alpha)^{\psi_3} - k_4 \mathrm{sig}(\alpha)^{\psi_4}, \\ \dot{\hat{d}} = -\lambda_3 \mathrm{sig}(\Omega)^{\psi_5} - \lambda_4 \mathrm{sig}(\Omega)^{\psi_6} - \lambda_5(t)\mathrm{sign}(\Omega), \end{cases} \tag{37}$$

where $\lambda_5(t)$ is updated by the following two-layer adaptive law:

$$\dot{\lambda}_5(t) = -(\varphi_0 + \varphi_1(t))\mathrm{sign}(\xi), \tag{38}$$

$$\dot{\varphi}_1(t) = \begin{cases} \varphi_d|\xi|, & |\xi| > \xi_0, \\ 0, & |\xi| \le \xi_0, \end{cases} \tag{39}$$

with

$$\begin{gathered} \xi = \lambda_5(t) - \frac{|\psi|}{\varepsilon_0} - \varepsilon_1, \\ \dot{\psi} = \eta \mathrm{fal}(-\lambda_5(t)\mathrm{sign}(\Omega) - \psi, \beta, \delta_0), \\ \mathrm{fal}(a, \beta, \delta_0) = \begin{cases} \mathrm{sig}(a)^{\beta}, & |a| > \delta_0, \\ \dfrac{a}{\delta_0^{1-\beta}}, & |a| \le \delta_0, \end{cases} \end{gathered} \tag{40}$$

where $k_3, k_4, \lambda_3, \lambda_4, \varphi_0, \varphi_d, \eta > 0$, $0 < \psi_3, \psi_5, \varepsilon_0, \varepsilon_1, \beta, \delta_0 < 1$, $\psi_4, \psi_6 > 1$, and $\tau > \sup(1, |\dot{\psi}|/D_1)$. If the parameters are chosen such that the following inequalities

$$\begin{gathered} \frac{|\psi|}{\varepsilon_0} + \frac{\varepsilon_1}{2} > |D_1|, \\ \xi_0^2 + \frac{\tau^2 D_1^2}{\varphi_d \varepsilon_0^2} < \frac{\varepsilon_1^2}{4}, \end{gathered} \tag{41}$$

hold, the observer error can converge to zero in finite time.

*Remark 3.* In [39], the proof for the stability of the adaptive disturbance observer was provided in detail.

**Theorem 2.** *For system (1), a novel composite controller by integrating the NNFTSMNDP method with ADO technique (NNFTSMNDP-ADO) is designed as*

$$u = -\frac{1}{b(x)}\left[a(x) + \hat{d} + \lambda_1 \mathrm{sig}(s)^{\kappa_1} + \lambda_2 \mathrm{sig}(s)^{\kappa_2} + \frac{1}{\gamma_2|x_2|^{\gamma_2-1}}\left(k_1' x_2 + \dot{k}_1' x_1 + k_2'\gamma_1|x_1|^{\gamma_1-1}x_2 + \dot{k}_2'\mathrm{sig}(x_1)^{\gamma_1}\right)\right], \tag{42}$$

*in which $\widehat{d}$ is the estimated disturbance by (37). Then, NNFTSM (5) can be reached in finite time. Furthermore, the system states can converge to the origin in finite time.*

*Proof*

*Step 1*. Consider a Lyapunov function $V_2 = 0.5s^2$, and its derivative is

$$\dot{V}_2 = s\dot{s} = s\left(k_1'x_2 + \dot{k}_1'x_1 + k_2'\gamma_1|x_1|^{\gamma_1-1}x_2 + \dot{k}_2'\mathrm{sig}(x_1)^{\gamma_1} + \gamma_2|x_2|^{\gamma_2-1}\dot{x}_2\right). \tag{43}$$

Substituting (42) into (43) yields

$$\begin{aligned}\dot{V}_2 = s\Big\{&k_1'x_2 + \dot{k}_1'x_1 + k_2'\gamma_1|x_1|^{\gamma_1-1}x_2 + \dot{k}_2'\mathrm{sig}(x_1)^{\gamma_1} - \gamma_2|x_2|^{\gamma_2-1}\Big[\widehat{d} + \frac{1}{\gamma_2|x_2|^{\gamma_2-1}}\left(k_2'x_2 + \dot{k}_1'x_1 + \dot{k}_2'\mathrm{sig}(x_1)^{\gamma_1}\right.\\ &\left.+ k_2'\gamma_1|x_1|^{\gamma_1-1}x_2\right) + \lambda_1\mathrm{sig}(s)^{\kappa_1} + \lambda_2\mathrm{sig}(s)^{\kappa_2} - d\Big]\Big\} = -s\gamma_2|x_2|^{\gamma_2-1}\left(\lambda_1\mathrm{sig}(s)^{\kappa_1} + \lambda_2\mathrm{sig}(s)^{\kappa_2} + \widehat{d} - d\right).\end{aligned} \tag{44}$$

Denote $e_d = \widehat{d} - d$; then,

$$\dot{V}_2 = -\gamma_2|x_2|^{\gamma_2-1}\left(\lambda_1|s|^{\kappa_1+1} + \lambda_2|s|^{\kappa_2+1} + e_d s\right). \tag{45}$$

From [39], it can be known that the observer error of ADO can converge to zero in finite time. It implies that there is a time constant $t^*$ satisfying that $e_d = 0$ for $t > t^*$. Define $t_r$ as the convergence time of the reaching motion. Select proper parameters for the reaching law and the observer to satisfy the condition $t_r > t^*$; then,

$$\dot{V}_2 = -\gamma_2|x_2|^{\gamma_2-1}\left(\lambda_1|s|^{\kappa_1+1} + \lambda_2|s|^{\kappa_2+1}\right). \tag{46}$$

For any $x_2 \neq 0$, since $V_2 > 0$ and $\dot{V}_2 < 0$, NNFTSM (5) can be reachable. Similar to the analysis before, $x_2 = 0$ does not hinder the reachability of NNFTSM. Substituting control law (42) into system (1), letting $x_2 = 0$, and ignoring the observer error $e_d = \widehat{d} - d$, it can be obtained that

$$\dot{x}_2 = -\lambda_1\mathrm{sig}(s)^{\kappa_1} - \lambda_2\mathrm{sig}(s)^{\kappa_2}. \tag{47}$$

When $x_1 > 0$, then $s > 0$, so $\dot{x}_2 < 0$. When $x_1 < 0$, then $s < 0$, so $\dot{x}_2 > 0$. It means that $x_2 = 0$ is not an attractor. Thus, it can be concluded that the reachability of NNFTSM (5) can be still guaranteed in the case of $x_2 = 0$.

The system trajectory can reach the sliding surface after a finite time, which is proved as follows.

Suppose $|s(0)| > 1$, and the reaching time $t_r$ can be estimated as

$$\int_0^{t_r}\mathrm{d}t = \int_0^{s(0)}\frac{1}{\lambda_1\mathrm{sig}(s)^{\kappa_1} + \lambda_2\mathrm{sig}(s)^{\kappa_2}}\mathrm{d}(s). \tag{48}$$

So,

$$\begin{aligned}t_r &< \int_1^{s(0)}\frac{1}{(\lambda_1+\lambda_2)\mathrm{sig}(s)^{\eta}}\mathrm{d}(s) + \int_0^1\frac{1}{\lambda_1\mathrm{sig}(s)^{\eta_2} + \lambda_2 s}\mathrm{d}(s) = \int_1^{s(0)}\frac{1}{(\lambda_1+\lambda_2)|s|^{\eta}}\mathrm{d}(|s|)\\ &+ \int_0^1\frac{1}{\lambda_1|s|^{\eta_2} + \lambda_2|s|}\mathrm{d}(|s|) = \frac{1-|s(0)|^{1-\eta}}{(\lambda_1+\lambda_2)(\eta-1)} + \frac{1}{\lambda_2(1-\eta_2)}\ln\left(1 + \frac{\lambda_2}{\lambda_1}\right).\end{aligned} \tag{49}$$

Thus, the system trajectory can converge to NNFTSM $s = 0$ in finite time.

*Step 2*. Consider a Lyapunov function $V_3 = 0.5x_1^2$; then, the time derivative of $V_3$ can be given by

$$\begin{aligned}\dot{V}_3 &= x_1\dot{x}_1\\ &= -x_1\left(k_1'|x_1| + k_2'|x_1|^{\gamma_1}\right)^{(1/\gamma_2)}\mathrm{sign}(x_1)\\ &< -\left(k_1'|x_1|\right)^{(1/\gamma_2)}|x_1| = -(k_1')^{(1/\gamma_2)}V_3^{((\gamma_2+1)/(2\gamma_2))}.\end{aligned} \tag{50}$$

According to Lemma 1, since $V_3 > 0$ and $\dot{V}_3 < 0$, the system states can be stabilized to the equilibrium point. The system states can arrive at the origin after a finite time, which is proved as follows.

Suppose $|x(0)| > \nu$, denote $t_s$ as the convergence time of the sliding motion, and it can be calculated as

$$\int_0^{t_s} \mathrm{d}t = \int_0^{x_1(0)} \frac{1}{\left(\left(2k_1/\left(1+e^{c_1(|x_1|-\nu)}\right)\right)|x_1| + \left(2k_2/\left(1+e^{-c_2(|x_1|-\nu)}\right)\right)|x_1|^{\gamma_1}\right)^{(1/\gamma_2)} \operatorname{sign}(x_1)} \mathrm{d}(x_1). \tag{51}$$

So,

$$\begin{aligned} t_s &= \int_\nu^{x_1(0)} \frac{1}{\left(\left(2k_1/\left(1+e^{c_1(|x_1|-\nu)}\right)\right)|x_1| + \left(2k_2/\left(1+e^{-c_2(|x_1|-\nu)}\right)\right)|x_1|^{\gamma_1}\right)^{(1/\gamma_2)}} \mathrm{d}(|x_1|) \\ &+ \int_0^\nu \frac{1}{\left(\left(2k_1/\left(1+e^{c_1(|x_1|-\nu)}\right)\right)|x_1| + \left(2k_2/\left(1+e^{-c_2(|x_1|-\nu)}\right)\right)|x_1|^{\gamma_1}\right)^{(1/\gamma_2)}} \mathrm{d}(|x_1|) \\ &< \int_\nu^{x_1(0)} \frac{1}{\left(k_2|x_1|^{\gamma_1}\right)^{(1/\gamma_2)}} \mathrm{d}(|x_1|) + \int_0^\nu \frac{1}{\left(k_1|x_1|\right)^{(1/\gamma_2)}} \mathrm{d}(|x_1|) = \frac{\gamma_2\left(|\nu|^{(1-(\gamma_1/\gamma_2))} - |x_1(0)|^{(1-(\gamma_1/\gamma_2))}\right)}{k_2^{(1/\gamma_2)}(\gamma_1-\gamma_2)} + \frac{\gamma_2|\nu|^{(1-(1/\gamma_2))}}{k_1^{(1/\gamma_2)}(\gamma_2-1)}. \end{aligned} \tag{52}$$

Thus, the system states can converge to origin in finite time. For system (1), the total convergence time of both the reaching motion and the sliding motion can be estimated as

$$t = t_r + t_s < \frac{1-|s(0)|^{1-\eta}}{(\lambda_1+\lambda_2)(\eta-1)} + \frac{1}{\lambda_2(1-\eta_2)} \ln\left(1+\frac{\lambda_2}{\lambda_1}\right) + \frac{\gamma_2\left(|\nu|^{(1-(\gamma_1/\gamma_2))} - |x_1(0)|^{(1-(\gamma_1/\gamma_2))}\right)}{k_2^{(1/\gamma_2)}(\gamma_1-\gamma_2)} + \frac{\gamma_2|\nu|^{(1-(1/\gamma_2))}}{k_1^{(1/\gamma_2)}(\gamma_2-1)}. \tag{53}$$

This completes the proof.

*Remark 4.* The disturbance observer error $e_d$ is ignored in (47). This is because the disturbance observer error can quickly converge to zero within finite time by designing proper parameters of ADO.

*Remark 5.* In the existence of external disturbances and parameter uncertainties, controller NNFTSMNDP-ADO can ensure the system states converge to the origin in finite time, while controller NNFTSMNDP drives the system states converge to the neighborhood of the origin in finite time. This is because the disturbance that is accurately observed by the ADO is feedforward compensated in the proposed controller in real-time.

## 4. Simulation Results

To verify the effectiveness and superiority of the proposed NNFTSMNDP-ADO control strategy, the section presents one study that is an application to a robotic manipulator control problem. The simulations are implemented based on the Matlab (R2014a)/Simulink. The dynamic equation of a two-link rigid robotic manipulator can be expressed as [43]

$$M(q)\ddot{q} + C(q,\dot{q})\dot{q} + G(q) = u + d, \tag{54}$$

with

$$M(q)=\begin{bmatrix}(m_1+m_2)l_1^2+m_2l_2^2+2m_2l_1l_2\cos(q_2)+J_1 & m_2l_2^2+m_2l_1l_2\cos(q_2)\\ m_2l_2^2+m_2l_1l_2\cos(q_2) & m_2l_2^2+J_2\end{bmatrix},$$
$$C(q,\dot{q})=\begin{bmatrix}-m_2l_1l_2\sin(q_2)\dot{q}_1 & -2m_2l_1l_2\sin(q_2)\dot{q}_1\\ 0 & m_2l_1l_2\sin(q_2)\dot{q}_2\end{bmatrix}, \tag{55}$$
$$G(q)=\begin{bmatrix}(m_1+m_2)gl_1\cos(q_2)+m_2gl_2\cos(q_1+q_2)\\ m_2gl_2\cos(q_1+q_2)\end{bmatrix},$$

in which $q_i$, $\dot{q}_i$, and $\ddot{q}_i$, respectively, stand for the vectors of joint position, velocity, and acceleration, $m_i$ denotes the link mass, $J_i$ denotes the link moment of inertia given in the centre of mass, and $u$ and $d$ are the control input and the external disturbance, respectively.

The system parameters of (55) are listed as follows:

$$\begin{aligned} m_1&=0.5\,\text{kg},\\ m_2&=1.5\,\text{kg},\\ l_1&=1\,\text{m},\\ l_2&=0.8\,\text{m},\\ J_1&=5\,\text{kg}\cdot\text{m}^2,\\ J_2&=5\,\text{kg}\cdot\text{m}^2,\\ g&=9.8\,\frac{\text{N}}{\text{s}^2}.\end{aligned} \tag{56}$$

The desired signals $q_d=[q_{1d},q_{2d}]^T$ can be described by

$$\begin{aligned} q_{1d}&=0.5e^{-4t}-1.2e^{-t}+1.25,\\ q_{2d}&=e^{-t}-0.5e^{-4t}+1.25.\end{aligned} \tag{57}$$

Consider the external disturbances $d=[d_1,d_2]^T$:

$$\begin{aligned} d_1&=2.5\cos(\pi t)+0.5\sin(2t),\\ d_2&=\sin(\pi t)+0.5\sin(2t).\end{aligned} \tag{58}$$

The initial states are set as follows: $q(0)=[1.5,0.5]^T$ and $\dot{q}(0)=[0,0]^T$.

Denoting $e_1=q-q_d$ and $e_2=\dot{q}-\dot{q}_d$, (54) can be converted to the following error equation:

$$\begin{cases}\dot{e}_1=e_2,\\ \dot{e}_2=a(e)+b(e)u+D,\end{cases} \tag{59}$$

where $a(e)=-M_0^{-1}(q)(C_0(q,\dot{q})\dot{q}+G_0(q))-\ddot{q}_d$, $b(e)=M_0^{-1}(q)$, and $D=-M_0^{-1}(q)(\Delta M(q)\ddot{q}+\Delta C(q,\dot{q})\dot{q}+\Delta G(q)-d)$.

In which, $M_0(q)$, $C_0(q,\dot{q})$, and $G_0(q)$ represent the nominal values and $\Delta M(q)$, $\Delta C(q,\dot{q})$, and $\Delta G(q)$ represent parameter perturbations.

*4.1. Robust Control.* According to Theorem 1, controller NNFTSMNDP is designed as follows:

$$\begin{aligned} u&=-M_0(q)\Big[\lambda_1\mathrm{sig}(s)^{\kappa_1}+\lambda_2\mathrm{sig}(s)^{\kappa_2}+a(e)+\left(\gamma_2|e_2|^{\gamma_2-1}\right)^{-1}\cdot\left(k_1'e_2+\dot{k}_1'e_1+k_2'\gamma_1|e_1|^{\gamma_1-1}e_2+\dot{k}_2'\mathrm{sig}(e_1)^{\gamma_1}\right)\Big],\\ s&=k_1'e_1+k_2'\mathrm{sig}(e_1)^{\gamma_1}+\mathrm{sig}(e_2)^{\gamma_2},\end{aligned} \tag{60}$$

where $s=[s_1,s_2]^T$, $\mathrm{sig}(e_1)^{\gamma_1}=[\mathrm{sig}(e_{11})^{\gamma_1},\mathrm{sig}(e_{12})^{\gamma_1}]^T$, $\mathrm{sig}(e_1)^{\gamma_2}=[\mathrm{sig}(e_{11})^{\gamma_2},\mathrm{sig}(e_{12})^{\gamma_2}]^T$, $\mathrm{sig}(s)^{\kappa_1}=[\mathrm{sig}(s_1)^{\kappa_{11}},\mathrm{sig}(s_2)^{\kappa_{12}}]^T$, and $\mathrm{sig}(s)^{\kappa_2}=[\mathrm{sig}(s_1)^{\kappa_{21}},\mathrm{sig}(s_2)^{\kappa_{22}}]^T$.

For comparison, a conventional nonsingular terminal sliding mode controller based on the double power reaching law (NFTSMDP) is designed as follows:

$$\begin{aligned} u&=-M_0(q)\Big[\lambda_1\mathrm{sig}(s)^{\psi_1}+\lambda_2\mathrm{sig}(s)^{\psi_2}+a(e)+\left(\beta\gamma_2|e_2|^{\gamma_2-1}\right)^{-1}\left(e_2+k\gamma_1|e_1|^{\gamma_1-1}e_2\right)\Big],\\ s&=e_1+k\mathrm{sig}(e_1)^{\gamma_1}+\beta\mathrm{sig}(e_2)^{\gamma_2}.\end{aligned} \tag{61}$$

The simulation parameters of the two controllers are set as $k_1 = k_2 = \mathrm{diag}\{1, 1\}$, $\beta = k = \mathrm{diag}\{1, 1\}$, $\gamma_1 = 2$, $\gamma_2 = 1.2$, $\lambda_1 = \lambda_2 = \mathrm{diag}\{3, 3\}$, $\eta = 2, \psi_1 = 0.6, \psi_2 = 2, \eta_0 = 1.8$, $\eta_1 = 0.4$, $\eta_2 = 0.6, r = 500, \theta = 800$.

By using the two controllers, the position tracking errors of joints 1 and 2 are illustrated in Figure 4. It is observed from Figure 4 that controller NNFTSMNDP obtains faster convergence rate and smaller steady-state tracking errors than controller NFTSMDP. Figure 5 shows the time responses of the sliding mode manifolds. It is clearly seen from Figure 5 that the time for the position tracking errors to reach the designed sliding mode manifolds is shorter under controller NNFTSMNDP compared to under controller NFTSMDP. Moreover, the sliding variable $s$ can converge to a smaller bounded region near zero under controller NNFTSMNDP. Thus, controller NNFTSMNDP has the faster convergence rate and higher tracking accuracy than controller NFTSMDP.

*4.2. External Disturbance Rejection.* According to (37), the adaptive disturbance observer is designed as

$$\begin{cases} \alpha = z - e_2, \\ \Omega = \dot{\alpha} + k_3 \mathrm{sig}(\alpha)^{\psi_3} + k_4 \mathrm{sig}(\alpha)^{\psi_4}, \\ \dot{z} = a(e) + \ddot{q}_d + b(e)u + \widehat{D} - k_3 \mathrm{sig}(\alpha)^{\psi_3} - k_4 \mathrm{sig}(\alpha)^{\psi_4}, \\ \dot{\widehat{D}} = -\lambda_3 \mathrm{sig}(\Omega)^{\psi_5} - \lambda_4 \mathrm{sig}(\Omega)^{\psi_6} - \lambda_5(t)\mathrm{sign}(\Omega), \end{cases} \tag{62}$$

where $\lambda_5(t)$ is updated by the adaptive law in (38).

According to Theorem 2 and combining observer (62), controller NNFTSMNDP-ADO is designed as

$$u = -M_0(q)\left[\lambda_1 \mathrm{sig}(s)^{\kappa_1} + \lambda_2 \mathrm{sig}(s)^{\kappa_2} + a(e) + \widehat{D} + \left(\gamma_2 |e_2|^{\gamma_2 - 1}\right)^{-1} \cdot \left(k_1' e_2 + \dot{k}_1' e_1 + k_2' \gamma_1 |e_1|^{\gamma_1 - 1} e_2 + \dot{k}_2' \mathrm{sig}(e_1)^{\gamma_1}\right)\right]. \tag{63}$$

The disturbances $d_1, d_2$ and the estimated disturbances $\widehat{d}_1, \widehat{d}_2$ are depicted in Figure 6. It can be seen that ADO can accurately observe the disturbances within finite time. Figure 7 shows the position tracking errors of joints 1 and 2 under controller NNFTSMNDP and controller NNFTSMNDP-ADO. It is obviously seen that the positions under controller NNFTSMNDP-ADO have no steady-state tracking errors, which confirms that the system states can converge to the equilibrium within finite time in Theorem 2. Figure 8 presents the time responses of the sliding mode manifolds under the two control schemes. It is noted that the sliding variable $s$ can converge to zero in finite time under controller NNFTSMNDP-ADO. This is because ADO can accurately estimate the external disturbances that are compensated in the controller in real-time. Therefore, the proposed NNFTSMNDP-ADO controller can achieve the higher tracking speed and better control precision in comparison with controller NNFTSMNDP.

*4.3. Robustness against Parameter Perturbation.* To further verify the robustness of controller NNFTSMNDP-ADO, the load variation of the robotic manipulator is considered in addition to the external disturbances. Suppose that the mass of joint 2 becomes 2.5 kg from 1.5 kg at 5 s. For comparison, controller NFTSMDP-ADO is designed by reference to the controller NNFTSMNDP-ADO design.

Figure 9 shows the tracking trajectories of joints 1 and 2 under controller NNFTSMNDP-ADO and controller NFTSMDP-ADO. Since NNFTSM and NDP decide a faster reaching and a faster sliding, it is observed from Figure 9 that the proposed NNFTSMNDP-ADO controller obtains faster tracking performance in comparison with controller

NFTSMDP-ADO: in the presence of parameter variation, the fluctuation of the position tracking errors under controller NNFTSMNDP-ADO are smaller in comparison with the fluctuation of the position tracking errors under controller NFTSMDP-ADO, as illustrated in Figure 10.

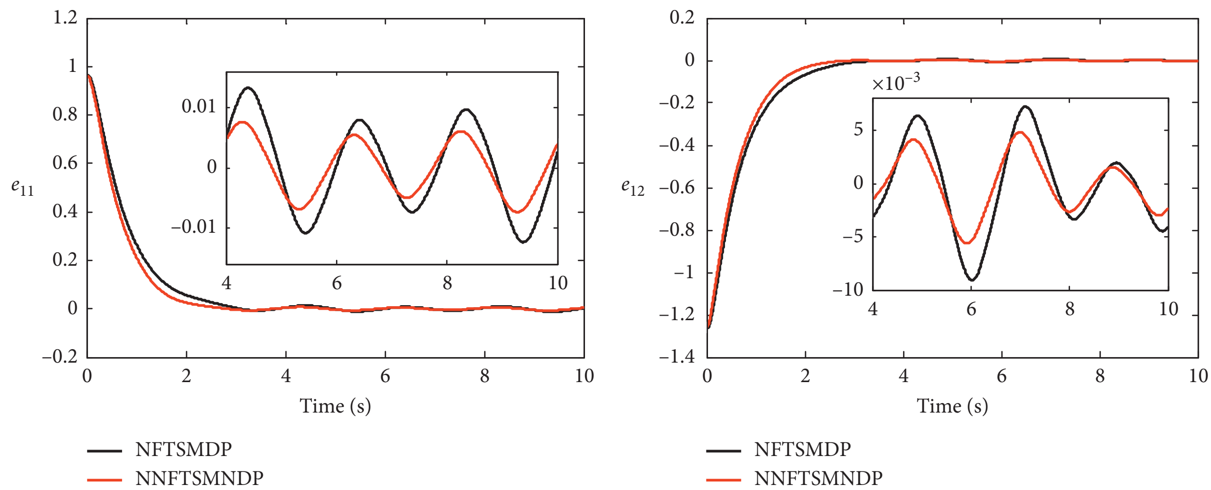


(a) (b)

Figure 4: The position tracking errors of joints 1 and 2 under controller NNFTSMNDP and controller NFTSMDP. (a) $e_{11}$. (b) $e_{12}$.

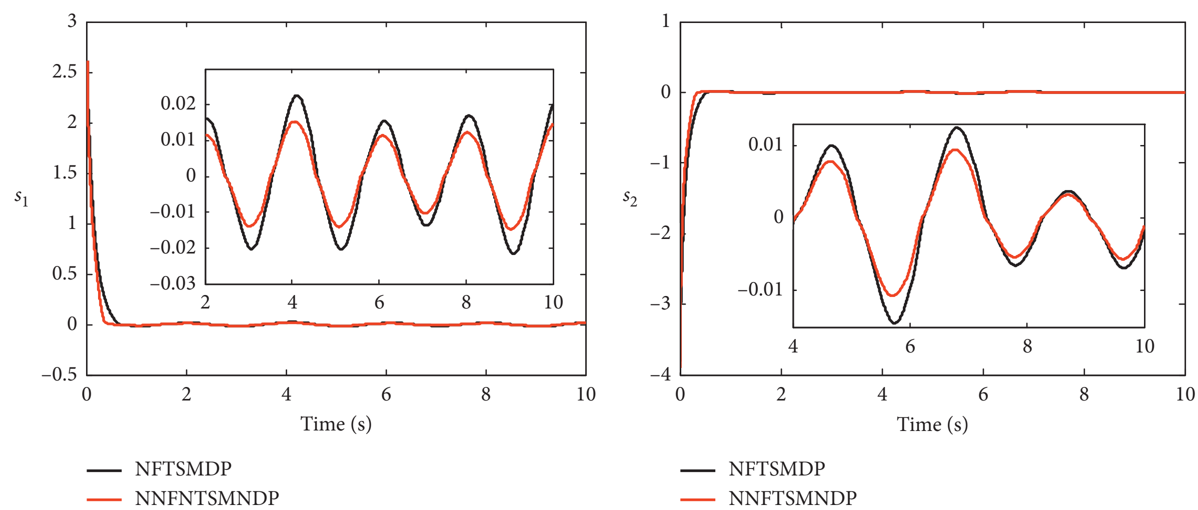


(a) (b)

Figure 5: Sliding surfaces versus time under controller NNFTSMNDP and controller NFTSMDP. (a) $s_1$. (b) $s_2$.

Moreover, in the existence of parameter perturbation, the recovery time for the position tracking errors convergence to zero is shorter under controller NNFTSMNDP-ADO. Thus, it can be concluded that the proposed NNFTSMNDP-ADO control technique can obtain the fine property of position recovery against parameter perturbation.

To better illustrate the superiority of the proposed NNFTSMNDP-ADO method, the other control scheme is also considered in simulation with the aim of comparison, which is the continuous nonsingular terminal sliding mode control method shown in [40]. According to [40], control law and observer are designed as

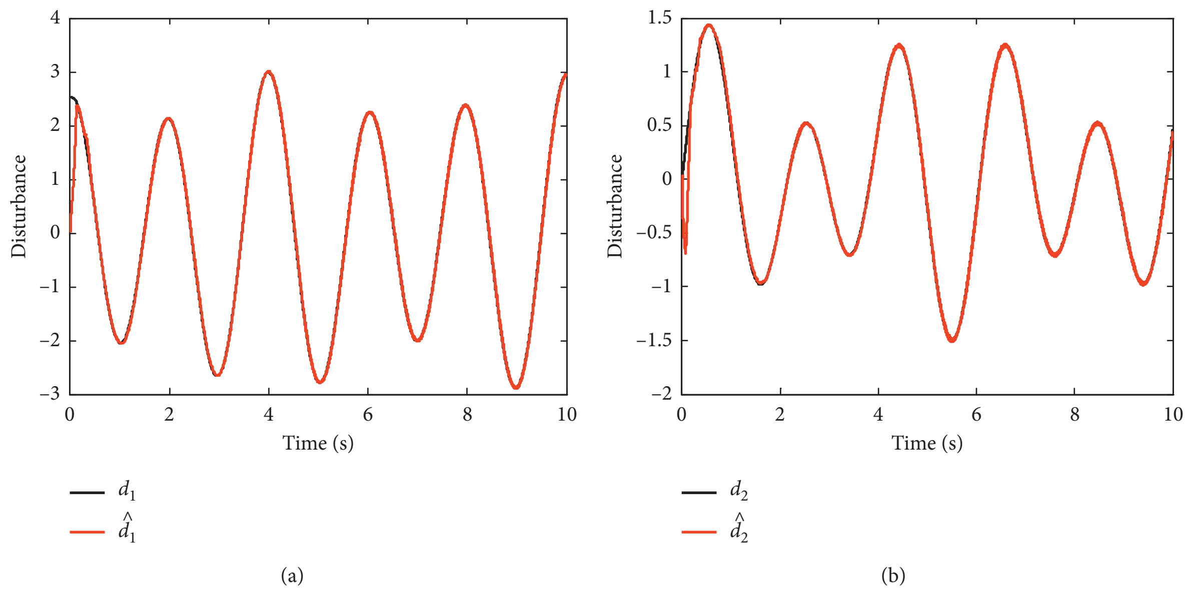


FIGURE 6: The disturbance and its estimation. (a) $d_1$ and its estimation. (b) $d_2$ and its estimation.

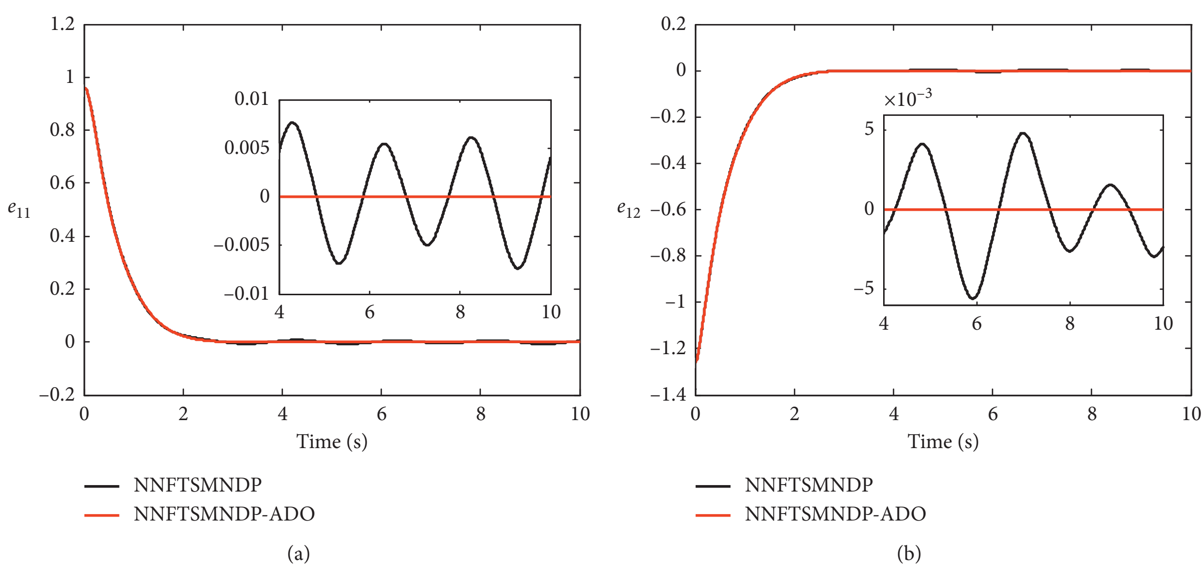


FIGURE 7: The tracking errors of joints 1 and 2 under controller NNFTSMNDP-ADO and controller NNFTSMNDP. (a) $e_{11}$. (b) $e_{12}$.

$$u = -M_0(q)\left(a(e) + l_1 \operatorname{sig}(e_1)^{\phi_1} + l_2 \operatorname{sig}(e_2)^{\phi_2} + \widehat{D}\right), \quad (64)$$

with

$$\begin{cases} \alpha = z - e_2, \\ \Omega = \dot{\alpha} + k_3 \operatorname{sig}(\alpha)^{\psi_3} + k_4 \operatorname{sig}(\alpha)^{\psi_4}, \\ \dot{z} = a(e) + \ddot{q}_d + b(e)u + \widehat{D} - k_3 \operatorname{sig}(\alpha)^{\psi_3} - k_4 \operatorname{sig}(\alpha)^{\psi_4}, \\ \dot{\widehat{D}} = -\lambda_5(t) \operatorname{sign}(\Omega), \end{cases} \quad (65)$$

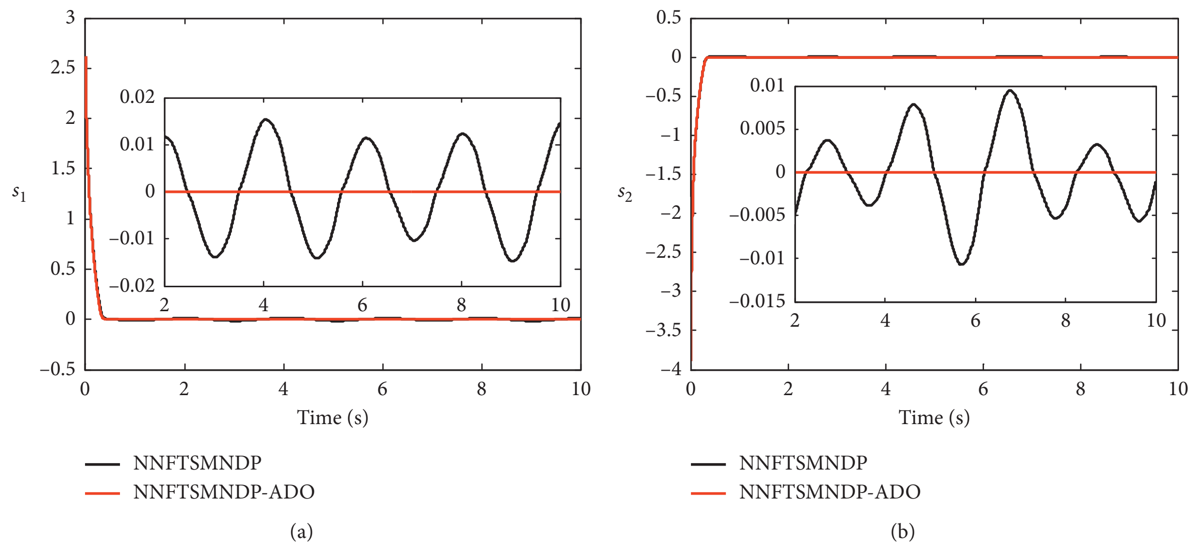


FIGURE 8: Sliding surfaces versus time under controller NNFTSMNDP-ADO and controller NNFTSMNDP. (a) $s_1$. (b) $s_2$.

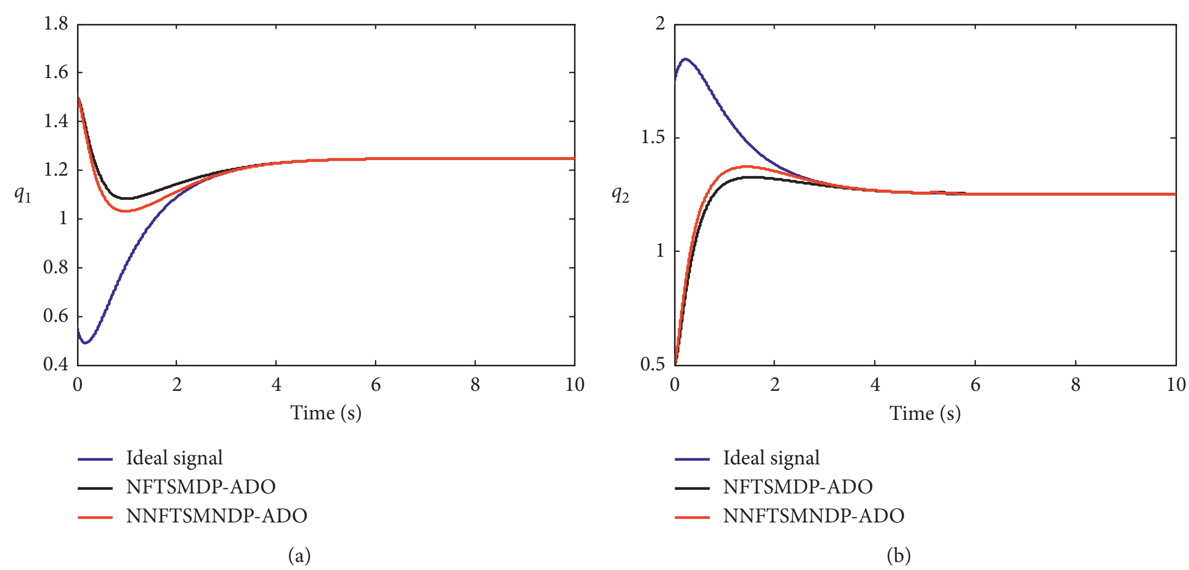


FIGURE 9: The tracking performances of joints 1 and 2 under controller NNFTSMNDP-ADO and controller NFTSMDP-ADO. (a) $q_1$. (b) $q_2$.

where $\lambda_5(t)$ is updated by (38). The parameters are set as $l_1 = l_2 = 5$, $\phi_2 = 0.8$, and $\phi_1 = (\phi_2/(2-\phi_2))$. The selection of the observer parameters is consistent with the parameter selection of ADO.

As shown in Figures 11 and 12, the comparative simulations are carried out with the same initial states given above in the presence of external disturbances and sudden load variation. From Figure 11, we can observe that the proposed NNFTSMNDP-ADO method provides the faster convergence than the method of [40]. Moreover, as shown in Figure 12, the proposed control method obtains the smaller perturbation and shorter recovery time for the tracking errors convergence to zero. The simulation results indicate the good control performance of the proposed method compared to the suggested method in [40].

All in all, controller NNFTSMNDP has better control performance than controller NFTSMDP. The position tracking errors under controller NNFTSMNDP-ADO can

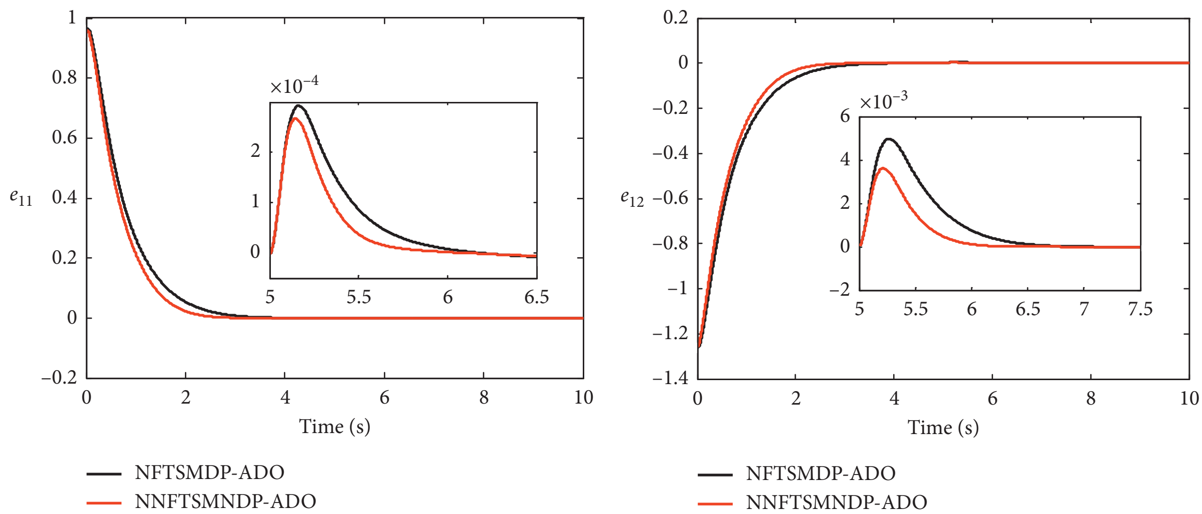


(a) (b)

Figure 10: The tracking errors of joints 1 and 2 under controller NNFTSMNDP-ADO and controller NFTSMDP-ADO. (a) $e_{11}$. (b) $e_{12}$.

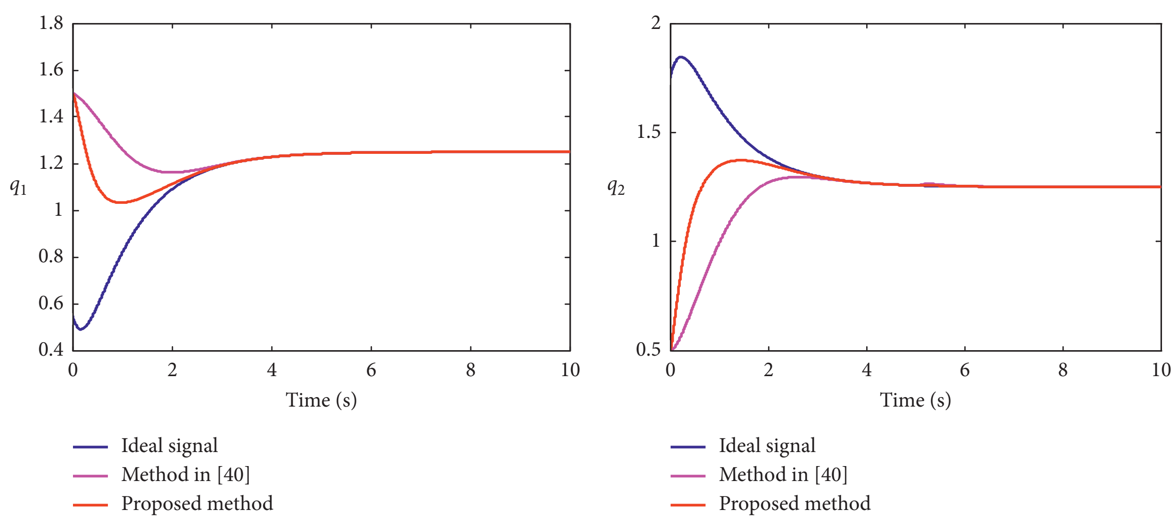


(a) (b)

Figure 11: The tracking performances of joints 1 and 2 under the proposed NNFTSMNDP-ADO method and the method in [40]. (a) $q_1$. (b) $q_2$.

converge to zero, while the position tracking errors under controller NNFTSMNDP can only converge to a small region near zero. Furthermore, the proposed NNFTSMNDP-ADO method can achieve faster convergence and better characteristic of position recovery against parameter uncertainties than NFTSMDP-ADO and the method of [40]. Thus, it can be concluded that the proposed NNFTSMNDP-ADO control scheme has the properties of fast finite-time

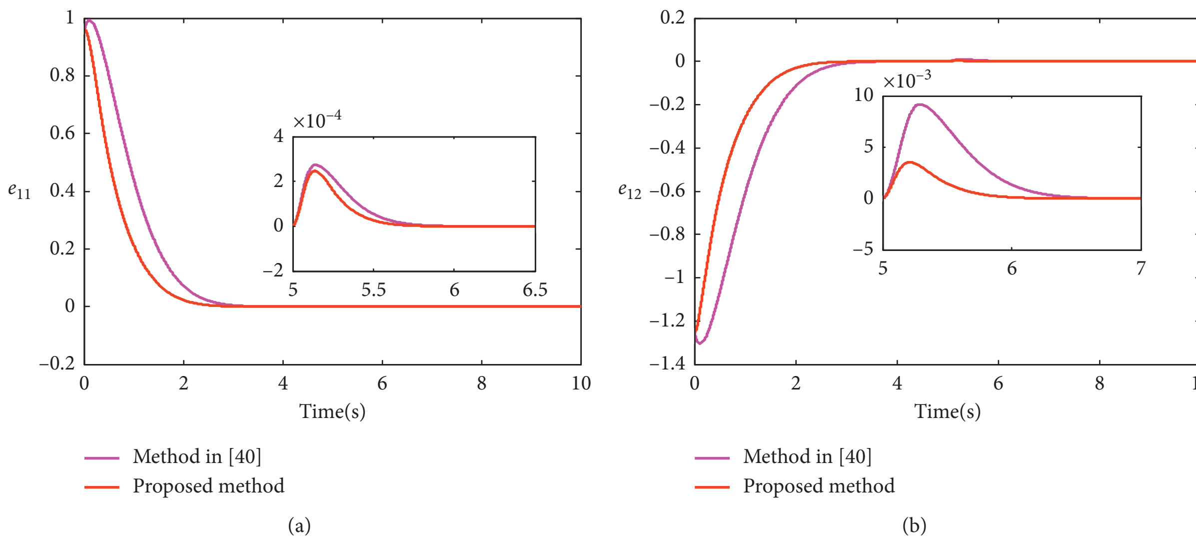


FIGURE 12: The tracking errors of joints 1 and 2 under the proposed NNFTSMNDP-ADO method and the method in [40]. (a) $e_{11}$. (b) $e_{12}$.

convergence, good tracking precision, and strong robustness.

## 5. Conclusions and Future Work

This paper proposes a novel NFTSM control method for a class of second-order uncertain nonlinear systems subject to disturbances and uncertainties. Firstly, a novel NFTSM and a novel DP are developed. Controller NNFTSMNDP is designed by combining NNFTSM and NDP, which has better control performance than controller NFTSMDP. However, under controller NNFTSMNDP, the system states cannot strictly converge to the equilibrium but only to the neighborhood of the equilibrium in finite time. To solve the problem, ADO is used to estimate the lumped disturbance that is compensated in the controller. Subsequently, a novel controller NNFTSMNDP-ADO involving NNFTSMNDP and ADO is proposed. The closed-loop system under the proposed composite controller guarantees both finite-time reachability to the sliding surface and finite-time stability of the system states to the equilibrium. Simulation results confirm that the proposed composite control approach can show excellent properties with respect to fast finite-time convergence, high control accuracy, and strong robustness. The proposed method is also applicable to control other second-order uncertain nonlinear systems. In the future, experiments will be conducted to further validate the proposed control strategy. In addition, we will focus on extending the proposed method to high-order uncertain nonlinear systems.

## Data Availability

The data used to support the findings of this study are available from the corresponding author upon request.

## Conflicts of Interest

The authors declare that there are no conflicts of interest.

## Acknowledgments

This work was supported by the National Natural Science Foundation of China (under grant no. 61703202) and by the Key Research Development Project of Jiangsu Province (under grant no. BE2017164).

## References


[1] J. Liu, Y. Zhao, B. Geng, and B. Xiao, “Adaptive second order sliding mode control of a fuel cell hybrid system for electric vehicle applications,” *Mathematical Problems in Engineering*, vol. 2015, Article ID 370424, 14 pages, 2015.

[2] S. Mobayen, “Fast terminal sliding mode controller design for nonlinear second-order systems with time-varying uncertainties,” *Complexity*, vol. 21, no. 2, pp. 239–244, 2015.

[3] S. Mobayen, “Design of LMI-based sliding mode controller with an exponential policy for a class of underactuated systems,” *Complexity*, vol. 21, no. 5, pp. 117–124, 2016.

[4] S. Ding, L. Liu, and W. X. Zheng, “Sliding mode direct yaw-moment control design for in-wheel electric vehicles,” *IEEE Transactions on Industrial Electronics*, vol. 64, no. 8, pp. 6752–6762, 2017.

[5] Y. Kali, M. Saad, K. Benjelloun, and A. Fatemi, “Discrete-time second order sliding mode with time delay control for uncertain robot manipulators,” *Robotics and Autonomous Systems*, vol. 94, pp. 53–60, 2017.

[6] H. Medhaffar and N. Derbel, “Fuzzy second-order sliding mode control design for a two-cell DC-DC converter,” *Mathematical Problems in Engineering*, vol. 2020, Article ID 1693971, 9 pages, 2020.

[7] S. Mobayen, F. Tchier, and L. Ragoub, “Design of an adaptive tracker forn-link rigid robotic manipulators based on super-

twisting global nonlinear sliding mode control," *International Journal of Systems Science*, vol. 48, no. 9, pp. 1990–2002, 2017.
[8] Y. Wang, K. Zhu, F. Yan, and B. Chen, "Adaptive super-twisting nonsingular fast terminal sliding mode control for cable-driven manipulators using time-delay estimation," *Advances in Engineering Software*, vol. 128, pp. 113–124, 2019.
[9] Q. Chen, S. Xie, M. Sun, and X. He, "Adaptive nonsingular fixed-time attitude stabilization of uncertain spacecraft," *IEEE Transactions on Aerospace and Electronic Systems*, vol. 54, no. 6, pp. 2937–2950, 2018.
[10] K. Zhao, T. Yin, C. Zhang et al., "Robust model-free nonsingular terminal sliding mode control for PMSM demagnetization fault," *IEEE Access*, vol. 7, pp. 15737–15748, 2019.
[11] X. Yu, M. Zhihong, and Y. Wu, "Terminal sliding modes with fast transient performance," in *Proceedings of the 1997 36th IEEE Conference on Decision and Control. Part 1 (of 5)*, vol. 2, pp. 962-963, San Diego, CA, USA, December 1997.
[12] L. Y. Wang, T. Y. Chai, and L. F. Zhai, "Neural-network-based terminal sliding mode control of robotic manipulators including actuator dynamics," *IEEE Transactions on Industrial Electronics*, vol. 56, no. 9, pp. 3296–3304, 2009.
[13] Z. Wang, Y. Su, and L. Zhang, "A new nonsingular terminal sliding mode control for rigid spacecraft attitude tracking," *Journal of Dynamic Systems Measurement and Control*, vol. 140, no. 5, 2018.
[14] S. Yu, X. Yu, B. Shirinzadeh, and Z. Man, "Continuous finite-time control for robotic manipulators with terminal sliding mode," *Automatica*, vol. 41, no. 11, pp. 1957–1964, 2005.
[15] M. L. Corradini and A. Cristofaro, "Nonsingular terminal sliding-mode control of nonlinear planar systems with global fixed-time stability guarantees," *Automatica*, vol. 95, pp. 561–565, 2018.
[16] L. Xin, Q. Wang, and Y. Li, "A new fast nonsingular terminal sliding mode control for a class of second-order uncertain systems," *Mathematical Problems in Engineering*, vol. 2016, Article ID 1743861, 12 pages, 2016.
[17] Y. Zhang, S. Tang, and J. Guo, "Adaptive terminal angle constraint interception against maneuvering targets with fast fixed-time convergence," *International Journal of Robust and Nonlinear Control*, vol. 28, no. 1, pp. 2996–3012, 2018.
[18] H. Liu, H. Wang, and J. Sun, "Attitude control for QTR using exponential nonsingular terminal sliding mode control," *Journal of Systems Engineering and Electronics*, vol. 30, no. 1, pp. 191–200, 2019.
[19] S. Mobayen, "Finite-time tracking control of chained-form nonholonomic systems with external disturbances based on recursive terminal sliding mode method," *Nonlinear Dynamics*, vol. 80, no. 1-2, pp. 669–683, 2015.
[20] S. Mobayen, "Fast terminal sliding mode tracking of nonholonomic systems with exponential decay rate," *IET Control Theory & Applications*, vol. 9, no. 8, pp. 1294–1301, 2015.
[21] H. Yan, X. Zhou, H. Zhang, F. Yang, and Z.-G. Wu, "A novel sliding mode estimation for microgrid control with communication time delays," *IEEE Transactions on Smart Grid*, vol. 10, no. 2, pp. 1509–1520, 2019.
[22] P. Gao, G. Zhang, H. Ouyang, and L. Mei, "A sliding mode control with nonlinear fractional order PID sliding surface for the speed operation of surface-mounted PMSM drives based on an extended state observer," *Mathematical Problems in Engineering*, vol. 2019, Article ID 7130232, 13 pages, 2019.
[23] P. Dai, N. Xu, H. Q. Xie, and L. Yan, "PMSM sliding mode control based on fast power reaching law," *Electric Machines and Control*, vol. 21, no. 11, pp. 32–38, 2017.
[24] Z. Zuo, "Non-singular fixed-time terminal sliding mode control of non-linear systems," *IET Control Theory & Applications*, vol. 9, no. 4, pp. 545–552, 2015.
[25] S. M. Mozayan, M. Saad, H. Vahedi, H. Fortin-Blanchette, and M. Soltani, "Sliding mode control of pmsg wind turbine based on enhanced exponential reaching law," *IEEE Transactions on Industrial Electronics*, vol. 63, no. 10, pp. 6148–6159, 2016.
[26] L. Tao, Q. Chen, Y. Nan, and C. Wu, "Double hyperbolic reaching law with chattering-free and fast convergence," *IEEE Access*, vol. 6, pp. 27717–27725, 2018.
[27] C. Xiu and P. Guo, "Global terminal sliding mode control with the quick reaching law and its application," *IEEE Access*, vol. 6, pp. 49793–49800, 2018.
[28] M. Tao, Q. Chen, X. He, and M. Sun, "Adaptive fixed-time fault-tolerant control for rigid spacecraft using a double power reaching law," *International Journal of Robust and Nonlinear Control*, vol. 29, no. 12, pp. 4022–4040, 2019.
[29] B. Brahmi, M. H. Laraki, A. Brahmi, M. Saad, and M. H. Rahman, "Improvement of sliding mode controller by using a new adaptive reaching law: theory and experiment," *ISA Transactions*, vol. 97, pp. 261–268, 2019.
[30] B. Kurkcu, C. Kasnakoglu, and M. O. Efe, "Disturbance/uncertainty estimator based integral sliding-mode control," *IEEE Transactions on Automatic Control*, vol. 63, no. 11, pp. 3940–3947, 2018.
[31] J. Yang, S. Li, C. Sun, and L. Guo, "Nonlinear-disturbance-observer-based robust flight control for airbreathing hypersonic vehicles," *IEEE Transactions on Aerospace and Electronic Systems*, vol. 49, no. 2, pp. 1263–1275, 2013.
[32] P. Xia, Y. Deng, Z. Wang, and H. Li, "Speed adaptive sliding mode control with an extended state observer for permanent magnet synchronous motor," *Mathematical Problems in Engineering*, vol. 2018, Article ID 6405923, 13 pages, 2018.
[33] J. Su, J. Yang, and S. Li, "Continuous finite-time anti-disturbance control for a class of uncertain nonlinear systems," *Transactions of the Institute of Measurement and Control*, vol. 36, no. 3, pp. 300–311, 2014.
[34] S. Li, J. Yang, W.-H. Chen, and X. Chen, "Generalized extended state observer based control for systems with mismatched uncertainties," *IEEE Transactions on Industrial Electronics*, vol. 59, no. 12, pp. 4792–4802, 2012.
[35] L. Zhou, Z. Che, and C. Yang, "Disturbance observer-based integral sliding mode control for singularly perturbed systems with mismatched disturbances," *IEEE Access*, vol. 6, pp. 9854–9861, 2018.
[36] S. Mobayen and F. Tchier, "Nonsingular fast terminal sliding-mode stabilizer for a class of uncertain nonlinear systems based on disturbance observer," *Scientia Iranica*, vol. 24, no. 3, pp. 1410–1418, 2017.
[37] N. P. Nguyen, H. Oh, Y. Kim, and J. Moon, "Disturbance observer-based continuous finite-time sliding mode control against matched and mismatched disturbances," *Complexity*, vol. 2020, Article ID 2085752, 14 pages, 2020.
[38] S. Mobayen, S. Mostafavi, and A. Fekih, "Non-singular fast terminal sliding mode control with disturbance observer for underactuated robotic manipulators," *IEEE Access*, vol. 8, pp. 198067–198077, 2020.
[39] H. Pan, G. Zhang, H. Ouyang, and L. Mei, "Novel fixed-time nonsingular fast terminal sliding mode control for second-order uncertain systems based on adaptive disturbance observer," *IEEE Access*, vol. 8, pp. 126615–126627, 2020.
[40] H. Rabiee, M. Ataei, and M. Ekramian, "Continuous nonsingular terminal sliding mode control based on adaptive

sliding mode disturbance observer for uncertain nonlinear systems," *Automatica*, vol. 109, pp. 1–7, 2019.

[41] S. P. Bhat and D. S. Bernstein, "Finite-time stability of continuous autonomous systems," *Siam Journal on Control and Optimization*, vol. 38, no. 3, pp. 751–766, 2000.

[42] A. Polyakov and L. Fridman, "Stability notions and Lyapunov functions for sliding mode control systems," *Journal of the Franklin Institute*, vol. 351, no. 4, pp. 1831–1865, 2014.

[43] L. Yang and J. Yang, "Nonsingular fast terminal sliding-mode control for nonlinear dynamical systems," *International Journal of Robust and Nonlinear Control*, vol. 21, no. 16, pp. 1865–1879, 2011.